THE JOURNAL OF PHYSICAL CHEMISTRY C
A JOURNAL OF THE AMERICAN CHEMICAL SOCIETY

pubs.acs.org/JPCC

Article

# 2D Missing Row Structure of Cuprous Fluoride on Cu(001)

M. N. Petukhov,* P. Krüger, A. I. Oreshkin, D. A. Muzychenko, and S. I. Oreshkin

Cite This: https://doi.org/10.1021/acs.jpcc.2c06295

Read Online

ACCESS | Metrics & More | Article Recommendations

**ABSTRACT:** Cuprous fluoride (CuF), unstable in bulk, can be stabilized as a two-dimensional lattice. Controlled adsorption of fluorine on the copper surface is achieved by defluorination of a self-assembled submonolayer of $C_{60}F_{18}$ molecules. The detached fluorine atoms diffuse on the Cu(001) surface and form a stable $(2\sqrt{2} \times \sqrt{2})R45°$ superstructure revealed by scanning tunneling microscopy. X-ray photoelectron spectroscopy indicates a chemisorption state of F atoms and an absence of Cu(II) oxidation state of surface copper atoms. Modeling with density functional theory shows that the unit cell contains three fluorine atoms corresponding to a missing row structure. This study proves the existence of surface cuprous fluoride.

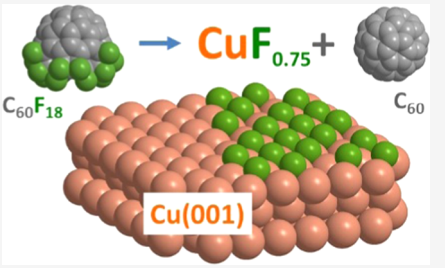




## INTRODUCTION

Two-dimensional (2D) metal halides have attracted a great interest for their tunable electronic, magnetic, and topological properties.[1,2] Copper halides are mainly stable components with a complex structure close to zinc blend. Copper(I) fluoride, in contrast to other cuprous halides, is recognized as unstable and nonisolable.[3] Although the synthesis of CuF was reported in 1957,[4] this result has never been reproduced. Nevertheless, possible existence of Cu(I) fluoride continues to be debated, especially in the theoretical literature.[5,6] On the basis of theoretical calculations, CuF has been predicted to have a Weyl semimetal band structure, which is of interest in physics and materials technology.[7] However, a reliable experimental description of the material is still absent. Indeed, CuF readily transforms into $CuF_2$ and Cu because of the exothermicity of its disproportionation reaction.[5] It has been shown that the single Cu−F bond in a solid state can be stabilized solely by the presence of other ligands.[8] However, standing alone CuF molecules and $(CuF)_n$ ($n$ = 3, 4) clusters have been detected in gas phase after sublimation from a hot polycrystalline Cu surface pre-exposed by fluorine beam.[9] This suggests that CuF might be stabilized in low-dimensional crystal structures. Nevertheless, only $CuF_2$ formation has been observed during thin-film growth on the copper surface after fluorination even by less aggressive $XeF_2$.[10] Such a complex behavior raises the study of fluorine atom adsorption on a copper surface as extremely challenging to establish the existence of CuF structures in the 2D case.

Moreover, even the interaction of single fluorine atoms with the copper surface is very poorly understood in comparison with other halogens.[11,12] The lack of detailed experimental studies of metal surface fluorination is partially caused by difficulties to work with reactive fluoride compounds and to dose a low concentration of fluorine atoms on the surface. It has been established that a thickness of thin fluoride films depends on a precursor molecule.[13] Therefore, the amount of adsorbed fluorine may be controlled by a suitable choice of the precursor. Recently, the fluorinated fullerene molecules ($C_{60}F_{18}$ and $C_{60}F_{48}$) have been proposed as precursors for F-induced surface structures on Cu(001).[14,15] When adsorbed at room temperature in submonolayer coverage, fluorinated fullerene molecules (FFM) form self-assembled 2D islands. Under the thermal effect, the FFM gradually lose their fluorine atoms on a time scale of hours until bare $C_{60}$ is reached.[14,16,17] After detachment from the FFM, the fluorine atoms diffuse on the surface region not covered by fullerenes and form F/Cu surface superstructures. The maximum amount of adsorbed fluorine on the surface is determined by the coverage and composition of the FFM precursor ($C_{60}F_{18}$ or $C_{60}F_{48}$). In the case of a submonolayer coverage of $C_{60}F_{18}$ molecules adsorbed at room temperature on Cu(001), F initially forms $c(2 \times 2)$ and $(\sqrt{17} \times \sqrt{17})R14°$ superstructures.[14] The latter structures are metastable and further transform into a $(2\sqrt{2} \times \sqrt{2})R45°$ lattice, which is very stable and could be observed by scanning tunneling microscopy (STM) for a week of continuous experiment. The atomic and electronic structure of the stable $(2\sqrt{2} \times \sqrt{2})R45°$ lattice has not yet been established.

Here, we use a $C_{60}F_{18}$ molecule as the precursor and study the F-induced $(2\sqrt{2} \times \sqrt{2})R45°$ superstructure on Cu(001) by scanning tunneling microscopy (STM), X-ray photoelectron spectroscopy (XPS), and first-principles calculations based on density functional theory (DFT).

Received: September 2, 2022
Revised: November 11, 2022

## EXPERIMENTAL AND THEORETICAL METHODS

The STM measurements were performed in an ultrahigh vacuum (UHV) chamber with a base pressure of $4 \times 10^{-11}$ mbar at room temperature. W tips were used for scanning, and image processing was done by WSxM software.[18] The XPS experiment was carried out in an UHV chamber with a base pressure of $1 \times 10^{-10}$ mbar equipped with an Omicron EA 125 hemispherical analyzer and XR705 VG Microtech X-ray source with a dual anode. The XPS spectra were obtained with Mg K$\alpha$ excitation and referenced to the Cu $2p_{3/2}$ peak of the clean copper surface at 932.7 eV of binding energy.[19] All spectra were acquired at the acceptance angle of 60° with respect to the surface normal. The STM images and XPS spectra were obtained at room temperature.

The clean surface of the Cu(001) crystal was prepared by cycles of argon ion sputtering (0.8−1.2 keV, 20 min), followed by annealing at 900 K. The cleaning cycles were repeated until a sharp pattern of a well-ordered $p(1 \times 1)$ structure of the surface was observed by a low-energy electron diffraction technique (Omicron SpectaLEED) or by STM. The $C_{60}F_{18}$ molecules were evaporated from a Knudsen cell on a clean copper surface kept at room temperature. The deposition rate 0.03−0.05 ML/min was used in the experiment. The submonolayer coverage of fluorinated fullerene close to 0.5 ML was principally examined. The defluorination process of FFM can continue for a week at room temperature.[14]

The XPS spectra acquisition at the angle of 60° with respect to the surface normal improves the surface sensitivity. The inelastic electron mean free path (IMFP) of Cu 2p photoelectrons in copper in this case is 3.5 Å according to Tanuma, Powell, and Penn algorithm TPP2M.[20] Hence, the measured Cu 2p spectrum corresponds to photoelectrons emitted from the two topmost atomic layers of the copper surface not covered by FFM. The Cu 2p photoelectrons emitted from the surface region covered by FFM islands are strongly attenuated as Cu 2p electrons with kinetic energy $E_k \leq 321$ eV have an IMFP of 6 Å in fullerenes, which is less than the diameter of a fullerene molecule.

Possible atomic structures of the observed $(2\sqrt{2} \times \sqrt{2})$R45°−F superstructure on Cu(001) were studied using DFT calculations. The projector-augmented wave code VASP was used with the PBE−GGA exchange−correlation functional. The energy cutoff was set to 400 eV. The Cu(001) substrate was modeled with a slab of six monolayers with a calculated fcc lattice constant of 3.634 Å (i.e., a Cu−Cu bond length of 2.57 Å). The lower copper layers were frozen in their bulk position, and the upper two were relaxed until the forces were below 0.01 eV/Å. Repeated Cu slabs were separated by 21 Å of vacuum. A Γ-centered $8 \times 16 \times 1$ $k$-point grid was used for the $(2\sqrt{2} \times \sqrt{2})$ cell. Total energies were corrected for the spurious dipole interaction between repeated slabs.

## RESULTS AND DISCUSSION

The STM images with a $(2\sqrt{2} \times \sqrt{2})$R45° structure in about 100 h after $C_{60}F_{18}$ deposition are shown in Figure 1. The superstructure grows between the fullerene self-assembled islands and covers a large area (>100 nm$^2$) of the copper crystal, as it can be seen in Figure 1a. The structure starts to appear in 48 h after fluorinated fullerene deposition at room temperature and has been traced by STM within 1 week of continuous experiment.[14] It has two domains with stripes along the ⟨110⟩ directions. The high-resolution image of the

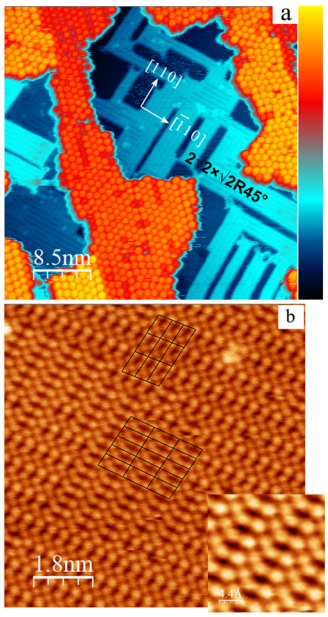


**Figure 1.** (a) STM images ($V_B$ = −2.2 V, $I_t$ = 18 pA) of $(2\sqrt{2} \times \sqrt{2})$R45° growth (blue color contrast) near the fullerene self-assembled island (yellow−red color contrast); (b) high-resolution STM topography image 9.2 × 9.2 nm$^2$ of $(2\sqrt{2} \times \sqrt{2})$R45° ($V_B$ = −60 mV, $I_t$ = 30 pA) with traced two domain orientation. A zoomed image with the stressed contrast of the central part is shown in the inset at the right bottom.

$(2\sqrt{2} \times \sqrt{2})$R45°−F superstructure with two domain orientation is shown in Figure 1b.

The XPS spectra of C 1s and F 1s lines and their time evolution after the deposition of the FFM on copper are shown in Figure 2. Previously, it has been shown that the C 1s XPS spectrum of the intact $C_{60}F_{18}$ molecule has a two-peak structure with peak positions at 288.7 and 285.7 eV corresponding to C atoms with and without a C−F bond, respectively.[21] In the meantime, the C 1s spectrum of bare $C_{60}$ has only one line at 284.7 eV.[21] The finding that the C 1s binding energy associated with the C atoms without a C−F bond differs by about 1 eV between FFM and pure $C_{60}$ can be understood as follows. When a fluorine atom is attached to the $C_{60}$, a redistribution of the molecular electron density occurs in the fullerene cage. This results in a chemical shift of the C−C bond to a higher binding energy, which is a function of the number of C−F bonds.[21,22]

The initial C 1s spectrum in Figure 2a has a complex structure with a high binding energy peak at 288.7 eV corresponding to C−F bonds and C−C states in $C_{60}$ and $C_{60}F_n$ at a lower binding energy of 284−286 eV. The FFM is not stable on the copper surface. Therefore, the defluorination of molecules starts immediately after the contact with the crystal surface. So, the initial C 1s spectrum in Figure 2a, obtained in 2 tens of minutes after deposition, eliminates the presence of both intact $C_{60}F_{18}$ molecules and decomposed FFM. The intensity of the C−F bond peak in Figure 2a decreases with time, suggesting a significant loss of fluorine by fullerene molecules after 44 h.

The large structure corresponding to the C−C bonds in fullerene molecules with $E_b$ = 284−286 eV develops with time into one dominating peak at $E_b$ = 284.6 eV (FWHM = 1.5 eV), approaching with time the state of the C−C bonds of bare $C_{60}$ on the Cu(001) (Figure 2a). The second component C−C


https://doi.org/10.1021/acs.jpcc.2c06295
J. Phys. Chem. C XXXX, XXX, XXX−XXX

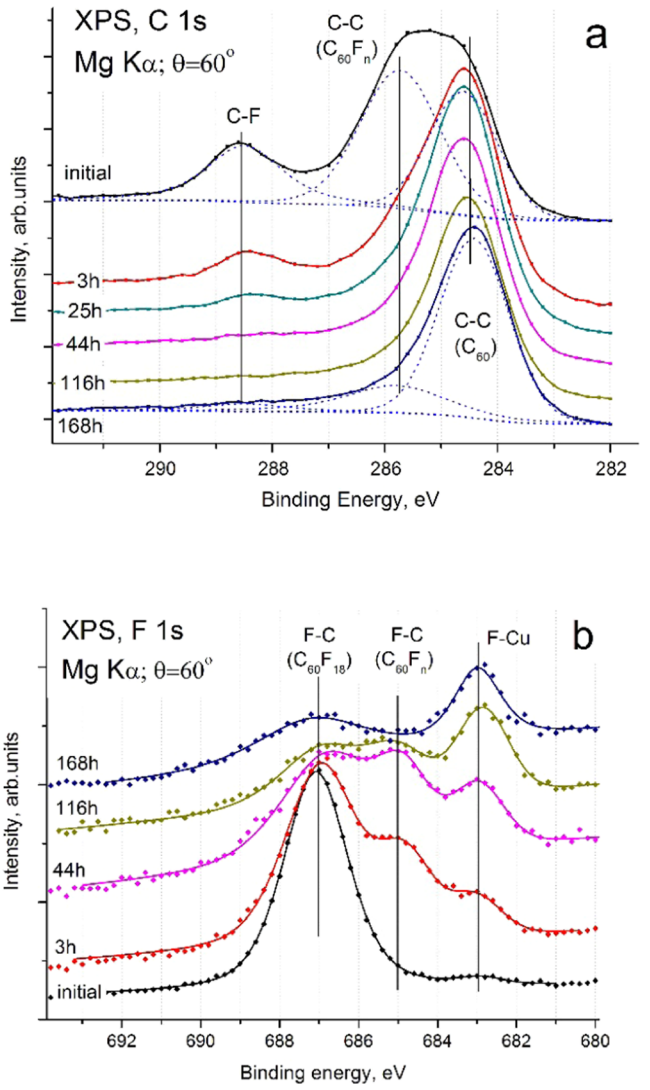


**Figure 2.** XPS spectra behavior with time (in hours) after $C_{60}F_{18}$ deposition. (a) C 1s spectra are presented as obtained; dotted lines show a peak fitting for initial and 168 h spectra by three components. (b) F 1s spectra are normalized and shifted for clarity. See also the text for the peak indication.

($C_{60}F_n$) of the structure decreases with time forming a high-energy shoulder of the dominating peak. The shape of late C 1s spectra indicates the presence of nondecomposed molecules on the surface. The peak fitting of the C 1s spectrum after 168 h estimates near 15% of FFM. A similar behavior of the C 1s spectra has been described in the case of $C_{60}F_{48}$ decomposition on the Cu(001) crystal.[22] By decomposing the C 1s spectra into three peaks, the degree of defluorination of FFM as a function of time can be estimated. The analysis method has been successfully used for the $C_{60}F_{48}$ molecule and described in detail before.[22]

The STM images of the FFM islands after a significant fluorine loss demonstrate a superstructure with the typical self-assembling of bare $C_{60}$ molecules on the Cu(001) surface.[14] This suggests that most of the FFM decompose to bare $C_{60}$. Assuming complete defluorination, we can estimate the number of fluorine atoms adsorbed on the copper surface. The area of the copper unit cell $S_U(Cu)$ equals to 6.6 Å$^2$/atom. The surface area covered by one FFM in the self-assembled islands $S_U(C_{60}F_n)$ equals to 105 Å$^2$/molecule in the self-assembled islands.[14] The ratio $18S_U(Cu)/S_U(C_{60}F_n) \approx 1$ is the value of the fluorine surface concentration after 1 ML of FFM coverage and complete defluorination of the molecules. This allows us to estimate the final concentration of fluorine atoms on the surface for 0.5 ML of initial FFM coverage close to 0.5 in the case of a homogeneous fluorine−copper surface interaction. However, the STM image analysis shows that the superstructure of self-assembled fullerene islands is close to bare $C_{60}$ on clean Cu(001) at the late stage of the defluorination process.[14] This fact can be explained either by an absence or by a reduced concentration of fluorine atoms under decomposed FFM islands. Hence, the detached fluorine atoms mainly interact with the noncovered copper surface. In the case of 0.5 ML of initial FFM coverage and preferred fluorination of noncovered copper surface, the fluorine concentration in the formed F-induced superstructure becomes greater than 0.5 and lower than 1.

The F 1s spectra of fluorinated fullerene molecules in Figure 2b have a complex structure and give an additional information on the surface fluorination process. The energy position of the F 1s line after FFM adsorption is 687.2 eV (FWHM = 1.9 eV), which is close to the literature data for intact $C_{60}F_{18}$.[21] This component of the spectra is marked as a F−C ($C_{60}F_{18}$) line in Figure 2b, and its intensity decreases with time. The other F−C bond component with binding energy around 685 eV appears in the spectra during the defluorination process. This F−C ($C_{60}F_n$) line is tentatively assigned to fluorine atoms of partially decomposed molecules $C_{60}F_n$, where $n < 18$, also interacting with copper. In a sense, this state is an interface state of fluorine between the fullerene cage and the substrate. A small shoulder appearance at a lower binding energy (683 eV) for the initial F 1s spectrum in Figure 2b specifies a start of surface-fluoride F−Cu bond formation. The intensity of the F−Cu chemical state grows with time and forms the sharp peak (FWHM = 1.3 eV) in the F 1s spectra at the late stage of the decomposition process.

In the final F 1s spectrum after 168 h in Figure 2b and later, only two components are present. The large line of F−C states at 687 eV of binding energy characterizes a part of FFM is still present on the surface and most probably passivated by defects and/or having a particular orientation of the molecule. The number of such molecules at the late stage of decomposition is near 15% as shows the peak fitting analysis of C 1s spectra. It is consistent with STM images of the previous study.[14] The lower binding energy 683 eV of the F 1s component corresponds to the fluorine atoms bound to the copper metal, i.e., forming a copper fluoride. It is worthwhile to note that this value of F 1s binding energy is at least 1 eV lower than that in the case of $CuF_2$, alkali metal fluorides, and metal fluoride glasses.[23−25]

The Cu 2p spectra obtained at the same time do not show any noticeable changes except the background inclination, see Figure 3. It is worthwhile to note that the Cu 2p signal in the chosen experimental conditions is mainly acquired from the surface not covered by FFM islands (see the experimental part). The Cu $2p_{3/2}$ peak located at 932.7 eV and the Cu $2p_{1/2}$ peak at 952.5 eV are always at the same position after molecule decomposition similar to the clean copper. The phenomenon of final-state splitting, typical in the case of $CuF_2$ formation, is absent.[22,23] The spectra after molecule adsorption have only a higher background impact in comparison with the Cu 2p spectrum of the clean copper surface.


https://doi.org/10.1021/acs.jpcc.2c06295
J. Phys. Chem. C XXXX, XXX, XXX−XXX

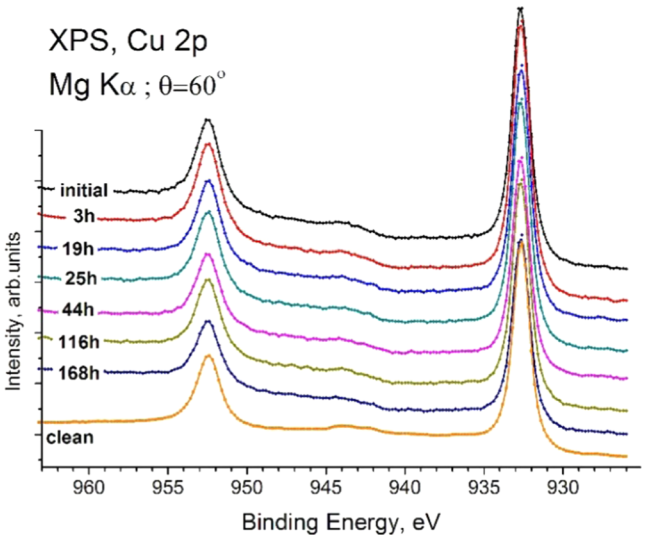


**Figure 3.** XPS Cu 2p spectra after $C_{60}F_{18}$ deposition on Cu(001) with time in comparison with the clean copper surface.

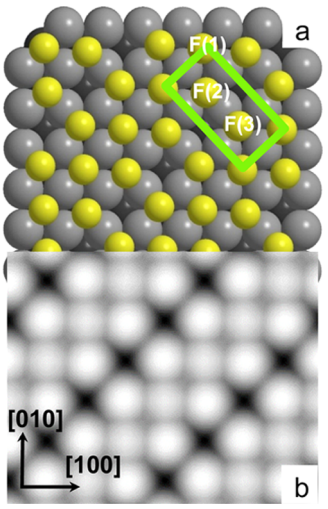


**Figure 4.** (a) Ball model of the $(2\sqrt{2} \times \sqrt{2})$R45°-3F superstructure. Yellow balls, fluorine atoms; gray balls, copper atoms of the last layer; and black balls, copper atoms of the near last layer. The unit cell is shown by green lines. (b) Corresponding simulated STM image of the superstructure (see also text). The image is lined with the atomic model of panel (a).

The spectra of other cuprous halides show the same behavior of the Cu 2p line. The Cu 2p spectra of CuI, CuBr, and CuCl have similar structure, and the Cu 2p binding energy values are close to the spectrum of the metal copper.[23,26−28] Evidently, the Cu 2p spectra in Figure 3 differ from the spectrum of $CuF_2$ and resemble the spectra of other cuprous halides. Therefore, we may conclude that the Cu(II) oxidation state of surface copper atoms is absent and the oxidation state formed on the copper surface after defluorination of 0.5 ML of FFM is close to Cu(I). It is important to note that $F_2$ formation can be excluded here. The $F_2$ dissociation energy is 1.6 eV/atom,[29] which is much lower than those of the F−Cu and F−C bond energies.

The model of the fluorine-induced superstructure $(2\sqrt{2} \times \sqrt{2})$R45° is based on the assumption that the first stage of the halogen interaction with metal surfaces is the chemisorption of halogen atoms.[11,12,30] The halogen−metal interaction is always a strong intermediate bond between ionic and covalent. In the case of fluorine, the interaction is rather ionic (charge between −0.6 and −0.8|e|).[31] For such an electronegative adsorbate, a direct repulsive dipole−dipole interaction plays a major role in the surface structure formation, and adatom repulsion on the surface is crucial.[12]

The simplest model of the $(2\sqrt{2} \times \sqrt{2})$R45° superstructure containing one adsorbed atom per unit cell corresponds to the fluorine surface concentration of 0.25. This value is too low in comparison with the estimation based on decomposition analysis. This is still true for the concentration of 0.5 with two fluorine atoms per unit cell. Moreover, any model with two F atoms per unit cell does not fit well the contrast of obtained STM images. An arrangement with three F atoms per $(2\sqrt{2} \times \sqrt{2})$R45° cell gives a realistic fluorine surface concentration of 0.75. From DFT calculations with this concentration, the structure in Figure 4a is found the most stable.

The superstructure in Figure 4a can be considered as a dense $p(1 \times 1)$ fluorine atom monolayer where one out of four [110] rows is missing. Other hypothetical superstructures with the same fluorine concentration, in particular, $p(2 \times 2)$−3F and $p(4 \times 1)$−3F structures, were found to be slightly less stable by 5−10 meV per F atom. This finding can be understood as follows. In all cases, the F atoms occupy the hollow sites, so the F−Cu interaction is the same. However, the number of nearest neighbor F−F pairs is different, and it is the lowest for the $(2\sqrt{2} \times \sqrt{2})$R45° structure. Since the ionic F−F interaction is repulsive, the structure with the lowest number of F−F bonds is most stable. The further increase of fluorine surface concentration to 1, i.e., formation of the $p(1 \times 1)$−F superstructure, seems impossible as the structure becomes unstable with regard to a surface atom rearrangement and thin-film growth as we have checked. In the DFT calculations, we have considered various other overlayer structures, and their systematic study will be published elsewhere. The proposed model superstructure $(2\sqrt{2} \times \sqrt{2})$R45°−3F is symmetrical with respect to the ⟨110⟩ directions and can have two domains similar to the domain orientation in the STM image in Figure 1b.

The calculated diffusion barrier of a single adsorbed fluorine atom is 38 meV. As this value is close to the thermal energy at room temperature, a high diffusion rate is expected, which explains the difficulty to observe the atomic structure of adsorbed fluorine at low coverage by STM at room temperature.[14] Adsorption energies are given in eV per F atom with reference to a single F atom in the gas phase. The calculated adsorption energy of the $(2\sqrt{2} \times \sqrt{2})$R45°−3F superstructure is 4.06 eV, which compares well with the value 4.22 eV, which was reported for F adsorption in the Cu(001) with coverage 0.125.[31] The literature adsorption energy for similar systems slightly varies around these values depending on coverage and copper crystal orientation.[31,32]

In the case of the $(2\sqrt{2} \times \sqrt{2})$R45°−3F superstructure of the present study, the four-fold hollow and near-hollow sites are found as the most favorable adsorption positions. The F(1) atom in the unit cell is placed in the hollow position, and F(2) and F(3) are shifted by 0.3 Å of the hollow site center, see Figure 4a. This lateral shift results in a F(2)−F(3) distance of 3.01 Å, i.e., 17% less than the theoretical distance between the corresponding hollow sites 3.63 Å of the copper surface. The F(1)−F(2) distance is 2.80 Å, which is 9% larger than the closest hollow site distance 2.57 Å on the Cu(001). Because of


https://doi.org/10.1021/acs.jpcc.2c06295
J. Phys. Chem. C XXXX, XXX, XXX−XXX

strong repulsion with neighboring adsorbates, F(2) and F(3) adatoms move to a more favorable location slightly higher above the surface (0.1 Å of vertical shift with respect to F(1)). Two adsorption sites for fluorine result in different closest distances with copper atoms. As the F(2) atom is displaced from the exact hollow site by 0.3 Å toward a top site and upward by 0.1 Å, the closest Cu−F(2) (and Cu−F(3)) distance 2.01 Å becomes shorter than the Cu−F(1) distance 2.15 Å.

The calculations also show that the fluorine adsorption does not result in significant structural changes of the metal substrate (vertical displacement is less than 0.05 Å for the surface copper layer) in agreement with the theoretical literature for lower F coverage and different copper crystal orientation.[31,32] However, at submonolayer coverage, the fluorine atoms repel each other and their interatomic distance depends on the F atom concentration.

In the stimulated STM contrast in Figure 4b, the fluorine atoms are seen like bright spots. The contrast of the constant current scan is formed by integrating the states from $E_F$ −0.1 eV to the Fermi level $E_F$. For the isodensity equal to $1 \times 10^{-5}$ e/Å$^3$, the black to white contrast in Figure 4b corresponds to the corrugation of 1.0 Å, which is in reasonable agreement with experimental corrugation 0.3 Å taking into account the tip shape effect. The variation of isodensity in 1 order of magnitude results in the same contrast of the image. So, the calculated pattern contrast in Figure 4b is independent of the tip height above the structure. Considering a possible thermal noise influence on the experimental STM images, the calculated pattern of Figure 4b describes well the observed experimental structure in Figure 1.

## CONCLUSIONS

Upon decomposition of a $C_{60}F_{18}$ submonolayer on Cu(001), a $(2\sqrt{2} \times \sqrt{2})$R45° phase of F/Cu(001) is formed, which is stable at room temperature. The atomic structure and chemical and electronic states of this phase have been analyzed by STM, XPS experiments, and DFT calculations. The fluorine coverage on the copper crystal is between 0.5 and 1 F atoms per Cu surface atom. The Cu 2p spectra analysis shows that the Cu surface atoms are not in the Cu(II) oxidation state but have a low valence. The DFT calculations support the proposed model of the surface superstructure $(2\sqrt{2} \times \sqrt{2})$R45°−3F with a formal stoichiometry $CuF_{0.75}$ and describe well the obtained STM images. The fluorine atoms of the structure are chemisorbed on the surface with a high adsorption energy of 4.06 eV/atom. This superstructure can be identified as the missing row cuprous fluoride structure. The results show that the interatomic F−F repulsion at submonolayer coverage stabilizes an ordered 2D structure on the copper monocrystal and prevents the disproportionation reaction of cuprous fluoride predicted in the bulk case.

## AUTHOR INFORMATION


### Corresponding Author

**M. N. Petukhov** − *ICB, UMR 6303 CNRS-Université de Bourgogne Franche-Comté, Dijon 21078, France;* orcid.org/0000-0002-1101-4163; Email: mikhail.petukhov@u-bourgogne.fr

### Authors

**P. Krüger** − *Graduate School of Engineering and Molecular Chirality Research Center, Chiba University, Chiba 263-8522, Japan;* orcid.org/0000-0002-1247-9886

**A. I. Oreshkin** − *Department of Physics, Lomonosov Moscow State University, Moscow 119991, Russia;* orcid.org/0000-0003-1342-2504

**D. A. Muzychenko** − *Department of Physics, Lomonosov Moscow State University, Moscow 119991, Russia;* orcid.org/0000-0002-1170-9491

**S. I. Oreshkin** − *Sternberg Astronomical Institute, Lomonosov Moscow State University, Moscow 119992, Russia*

Complete contact information is available at: https://pubs.acs.org/10.1021/acs.jpcc.2c06295


### Notes

The authors declare no competing financial interest.

## ACKNOWLEDGMENTS

This research was funded in part by project RSF N 22-22-00571.

## REFERENCES


(1) Hu, Y.; Guo, Y.; Wang, Y.; Chen, Z.; Sun, X.; Feng, J.; Lu, T-M.; Wertz, E.; Shi, J. A review on low dimensional metal halides: Vapor phase epitaxy and physical properties. *J. Mater. Res.* **2017**, *32*, 3992−4023.

(2) Huang, X.; Yan, L.; Zhou, Y.; Wang, Y.; Song, H-Z.; Zhou, L. Group 11 Transition-Metal Halide Monolayers: High Promises for Photocatalysis and Quantum Cutting. *J. Phys. Chem. Lett.* **2021**, *12*, 525−531.

(3) Shibasaki, M.; Kanai, M. Copper(I) Fluoride and Copper(II) Fluoride. In *Encyclopedia of Reagents for Organic Synthesis*; Paquette, L. A., Ed.; John Willey & Sons, Ltd., 2007; Vol. *8*.

(4) Mccaulay, D. A. Preparation of Cuprous FluorideU.S. Patent US2,817,576A, 1957.

(5) Walsh, A.; Catlow, C. R. A.; Galvelis, R.; Scanlon, D. O.; Schiffmann, F.; Sokol, A. A.; Woodley, S. M. Prediction on the Existence and Chemical Stability of Cuprous Fluoride. *Chem. Sci.* **2012**, *3*, 2565−2569.

(6) Kuklin, M. S.; Maschio, L.; Usvyat, D.; Kraus, F.; Karttunen, A. J. Evolutionary Algorithm-Based Crystal Structure Prediction for Copper(I) Fluoride. *Chem. - Eur. J.* **2019**, *25*, 11528−11537.

(7) Du, Y.; Kan, E.; Xu, H.; Savrasov, S. Y.; Wan, X. Turning Copper Metal into a Weyl Semimetal. *Phys. Rev. B* **2018**, *97*, No. 245104.

(8) Gulliver, D. J.; Levason, W.; Webster, M. Coordination Stabilized Copper(I) Fluoride. Crystal and Molecular Structure of Fluorotris(triphenylphosphine)copper(I) Ethanol(1/2), $Cu(PPh_3)3F$-2EtOH. *Inorg. Chim. Acta* **1981**, *52*, 153−159.

(9) Sugawara, K.; Wach, T.; Wanner, J.; Jakob, P. Desorption Kinetics of Copper Fluorides in the Reaction of Fluorine with Copper Surfaces. *J. Chem. Phys.* **1995**, *102*, 544−550.

(10) Qiu, S. R.; Yarmoff, J. A. Self-limiting Growth of Transition-metal Fluoride Films from the Reaction with $XeF_2$. *Phys. Rev. B* **2001**, *63*, No. 115409.

(11) Jones, R. G. Halogen Adsorption on Solid Surfaces. *Prog. Surf. Sci.* **1988**, *27*, 25−160.

(12) Andryushechkin, B. V.; Pavlova, T. V.; Eltsov, K. N. Adsorption of Halogens on Metal Surfaces. *Surf. Sci. Rep.* **2018**, *73*, 83−115.

(13) Qiu, S. R.; Lai, H.-F.; Yarmoff, J. A. Self-Limiting Growth of Metal Fluoride Thin Films by Oxidation Reactions Employing Molecular Precursors. *Phys. Rev. Lett.* **2000**, *85*, 1492−1495.

(14) Oreshkin, A. I.; Muzychenko, D. A.; Oreshkin, S. I.; Yakovlev, V. A.; Murugan, P.; Chandrasekaran, S. S.; Kumar, V.; Bakhtizin, R. Z. Real-Time Decay of Fluorinated Fullerene Molecules on Cu (001)

Surface Controlled by Initial Coverage. *Nano Res.* **2018**, *11*, 2069−2082.
(15) Oreshkin, A. I.; Muzychenko, D. A.; Oreshkin, S. I.; Panov, V. I.; Bakhtizin, R. Z.; Petukhov, M. N. Fluorinated Fullerene Molecule on Cu(001) Surface as a Controllable Source of Fluorine Atoms. *J. Phys. Chem. C* **2018**, *122*, 24454−24458.
(16) Palacios-Rivera, R.; Malaspina, D. C.; Tessler, N.; Solomeshch, O.; Faraudo, J.; Barrena, E.; Ocal, C. Surface specificity and mechanistic pathway of de-fluorination of $C_{60}F_{48}$ on coinage metals. *Nanoscale Adv.* **2020**, *2*, 4529−4538.
(17) Barrena, E.; Palacios-Rivera, R.; Babuji, A.; Schio, L.; Tormen, M.; Floreano, L.; Ocal, C. On-surface products from de-fluorination of $C_{60}F_{48}$ on Ag(111): $C_{60}$, $C_{60}F_x$ and silver fluoride formation. *Phys. Chem. Chem. Phys.* **2022**, *24*, 2349−2356.
(18) Horcas, I.; Fernández, R.; Gomez-Rodriguez, J.; Gómez-Rodríguez, J. M.; Colchero, J.; Colchero, J.; Gomez-Herrero, J.; Gómez-Herrero, J.; Baro, A. WSXM: A software for scanning probe microscopy and a tool for nanotechnology. *Rev. Sci. Instrum.* **2007**, *78*, No. 013705.
(19) Seah, M. P. Post-1989 Calibration Energies for X-ray Photoelectron Spectrometers and the 1990 Josephson Constant. *Surf. Interface Anal.* **1989**, *14*, No. 488.
(20) Tanuma, S.; Powell, C. J.; Penn, D. R. Calculations of electron inelastic mean free paths. V. Data for 14 organic compounds over the 50 - 2000 eV range. *Surf. Interface Anal.* **1994**, *21*, 165−176.
(21) Mikoushkin, V. M.; Shnitov, V. V.; Bryzgalov, V. V.; Gordeev, Yu.S.; Boltalina, O. V.; Gol'dt, I. V.; Molodtsov, S. L.; Vyalikh, D. V. Core Electron Level Structure in $C_{60}F_{18}$ and $C_{60}F_{36}$ Fluorinated Fullerenes. *Tech. Phys. Lett.* **2009**, *35*, 256−259.
(22) Petukhov, M. N.; Oreshkin, A. I.; Muzychenko, D. A.; Oreshkin, S. I. Fluorination of Cu(001) Surface by $C_{60}F_{48}$ Molecules Adsorption. *J. Phys. Chem. C* **2020**, *124*, 347−355.
(23) Biesinger, M. C. Advanced Analysis of Copper X-ray Photoelectron Spectra. *Surf. Interface Anal.* **2017**, *49*, 1325−1334.
(24) Morgan, W. E.; Van Wazer, J. R.; Stec, W. J. Inner-Orbital Photoelectron Spectroscopy of the Alkali Metal Halides, Perchlorates, Phosphates, and Pyrophosphates. *J. Am. Chem. Soc.* **1973**, *95*, 751−755.
(25) Kawamoto, Y.; Ogura, K.; Shojiya, M.; Takahashi, M.; Kadono, K. F1s XPS of Fluoride Glasses and Related Fluoride Crystals. *J. Fluorine Chem.* **1999**, *96*, 135−139.
(26) Vasquez, R. P. CuCl by XPS. *Surf. Sci. Spectra* **1993**, *2*, 138−143.
(27) Vasquez, R. P. CuBr by XPS. *Surf. Sci. Spectra* **1993**, *2*, 144−148.
(28) Vasquez, R. P. CuCl by XPS. *Surf. Sci. Spectra* **1994**, *2*, 149−154.
(29) Csontos, B.; Nagy, B.; Csontos, J.; Kállay, M. Dissociation of the Fluorine Molecule. *J. Phys. Chem. A* **2013**, *117*, 5518−5528.
(30) Altman, E. I. Halogens on Metals and Semiconductors. In *Adsorbed Layers on Surfaces. Part 1: Adsorption on Surfaces and Surface Diffusion of Adsorbates*; Bonzel, A. P., Ed.; Springer: Berlin, 2001; pp 420−442.
(31) Migani, A.; Illas, F. A Systematic Study of the Structure and Bonding of Halogens on Low-Index Transition Metal Surfaces. *J. Phys. Chem. B* **2006**, *110*, 11894−11906.
(32) Pašti, I. A.; Gavrilov, N. M.; Mentus, S. V. Fluorine Adsorption on Transition Metal Surfaces − A DFT Study. *J. Serb. Chem. Soc.* **2013**, *78*, 1763−1773.


https://doi.org/10.1021/acs.jpcc.2c06295
*J. Phys. Chem. C* XXXX, XXX, XXX−XXX